



**HAL**  
open science

# Development of an experimental bench to reproduce the tow buckling defect appearing during the complex shape forming of structural flax based woven composite reinforcements

Christophe Tephany, Jean Gillibert, Pierre Ouagne, Gilles Hivet, Samir Allaoui, Damien Soulat

## ► To cite this version:

Christophe Tephany, Jean Gillibert, Pierre Ouagne, Gilles Hivet, Samir Allaoui, et al.. Development of an experimental bench to reproduce the tow buckling defect appearing during the complex shape forming of structural flax based woven composite reinforcements. *Composites Part A: Applied Science and Manufacturing*, 2016, 81, pp.22-33. 10.1016/j.compositesa.2015.10.011 . hal-02135760

**HAL Id: hal-02135760**

**<https://hal.science/hal-02135760>**

Submitted on 21 May 2019

**HAL** is a multi-disciplinary open access archive for the deposit and dissemination of scientific research documents, whether they are published or not. The documents may come from teaching and research institutions in France or abroad, or from public or private research centers.

L'archive ouverte pluridisciplinaire **HAL**, est destinée au dépôt et à la diffusion de documents scientifiques de niveau recherche, publiés ou non, émanant des établissements d'enseignement et de recherche français ou étrangers, des laboratoires publics ou privés.



## Open Archive Toulouse Archive Ouverte (OATAO)

OATAO is an open access repository that collects the work of Toulouse researchers and makes it freely available over the web where possible

This is an author's version published in: <http://oatao.univ-toulouse.fr/23349>

**Official URL:** <https://doi.org/10.1016/j.compositesa.2015.10.011>

**To cite this version:**

Tephany, Christophe and Gillibert, Jean and Ouagne, Pierre and Hivet, Gilles and Allaoui, Samir and Soulat, Damien *Development of an experimental bench to reproduce the tow buckling defect appearing during the complex shape forming of structural flax based woven composite reinforcements.* (2016) *Composites Part A: Applied Science and Manufacturing*, 81. 22-33. ISSN 1359-835X

Any correspondence concerning this service should be sent to the repository administrator: [tech-oatao@listes-diff.inp-toulouse.fr](mailto:tech-oatao@listes-diff.inp-toulouse.fr)

# Development of an experimental bench to reproduce the tow buckling defect appearing during the complex shape forming of structural flax based woven composite reinforcements

C. Tephany<sup>a</sup>, J. Gillibert<sup>a</sup>, P. Ouagne<sup>a,\*</sup>, G. Hivet<sup>a</sup>, S. Allaoui<sup>a</sup>, D. Soulat<sup>b</sup>

<sup>a</sup>Univ. Orléans, PRISME EA4229, F-45072 Orléans, France

<sup>b</sup>GEMTEX, ENSAIT Roubaix 2 allée Louise et Victor Champier, 59056 Roubaix, France

## A B S T R A C T

This work investigates the tow buckling defect that may take place during the forming of complex shapes. The defect is studied independently of the process with a device specially designed. A specific instrumentation was associated to the device. Structure light interferometry was chosen to measure the elevation of the tows exhibiting the buckling defect all along its growth. The device and its instrumentation were validated in this work and a preliminary study was performed to investigate the origin of the tow buckle's appearance and its growth kinematic. The growth kinematic of the buckle's appearance consisting on a double simultaneous rotation of the tow exhibiting the buckle around the Z and the Y axis was established. It was shown that the in-plane bending of the tow is a key parameter that can probably be considered as a preliminary criterion that conditions the appearance and the growth of the tow buckling defect.

## Keywords:

A. Tow  
B. Defects  
E. Preform  
A. Fabrics/textiles

## 1. Introduction

The manufacturing of complex shape composites requires a step of preforming of the reinforcement. During the RTM (Resin Transfer Moulding), or vacuum infusion processes, the dry textile is formed on metallic tools. This is also the case for the prepreg or commingled reinforcement forming processes during which the resin already closely integrated into the fabric needs to be brought above its fusion temperature [1,2]. During this preforming step it is important to control the fibre orientation and the local density of the fabric to avoid fibre misalignments or defects which would reduce the mechanical properties of the composite part. Since 2013, several papers have completed the review article published in 2013 by Gereke et al. [3] on this subject. These recent papers deal with the subject of the multilayers forming [4] associated to the analysis of sliding between plies [5] and/or contact with tools [6]. The forming step of specific materials such as the ones based on natural fibres [7,8], or specific textile architecture such as non-crimped fabrics (NCF) [9] or 3D-interlock [10] is also described. Numerical approaches for the modelling of this step are also the subject of recent papers [9,11,12]. All these papers

demonstrate the large effort which is undertaken to understand the textile behaviour during forming, and especially the link between the physical and mechanical properties with defect that may appear. Several classical preforming defects may lead to an unsuccessful draping. As an example, it is possible to investigate at the scale of the preform if the expected shape is well obtained (if the preform fits to the tool), if wrinkle defects appear [13–17], if there is non-homogeneity of the reinforcement density, or if a loss of cohesion of the woven fabric appears [18]. At the scale of the tows other defects may appear. Tow misalignment in the plane of the fabric [19], or out-of-plane misalignment also called tow buckles [8,9,17] have been identified and investigated. All these defects have a strong influence on the resin flow impregnation because they modify the pore space within the fabric and therefore the in-plane and through-the thickness permeability components [20–23]. All these defects were initially detected and investigated by using experimental approaches conducted on preforming device and especially on complex shapes. The development of preforming numerical models requires the definition of the reinforcement behaviour laws [24] but also requires the identification of criteria to predict the appearance of defects. Specific elementary tests may be developed to investigate the parameters that control the appearance of a given defect. These tests may also be used to elaborate solutions to prevent them. The most widely used test is

\* Corresponding author.

E-mail address: pierre.ouagne@univ-orleans.fr (P. Ouagne).

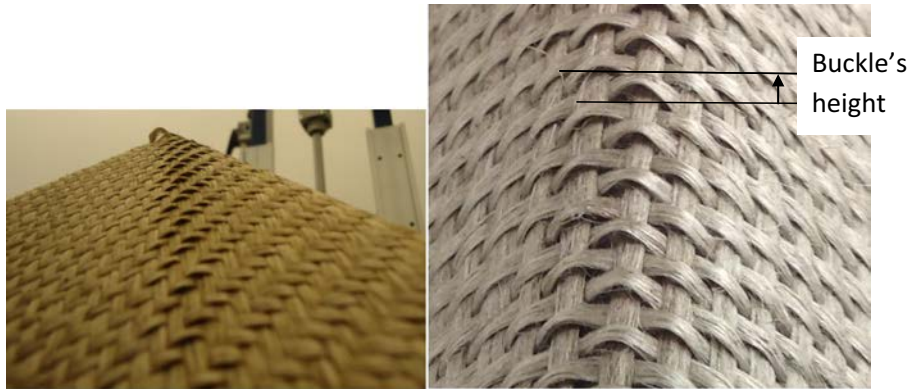


**Fig. 1.** Tow buckling phenomenon on the face and on one edge of a tetrahedron shape. (For interpretation of the references to colour in this figure legend, the reader is referred to the web version of this article.)

the in-plane shear test to detect the locking shear angle [25,26] associated to the wrinkling defect. For the in-plane shear behaviour and the identification of the locking shear angle, bias-tests or picture-frame tests can be conducted [27]. The determination of the tensile [28,29], bending [2,30], friction [31–33] behaviours or the identification of the permeability [21,34] are commonly used to identify limits of behaviour, independently of the preforming process. Due to the difficulty to identify all the causes leading to the appearance of the tow buckling defect, this paper proposes to study it independently of the process by using a specially designed experimental bench.

In this paper, a complete description of an instrumented device capable of reproducing independently of the forming process the tow buckling phenomenon, coupled to a non-contact method to detect the appearance and measure the size of the defect with accuracy is presented. The first preliminary results are commented and analysed. In a second step of this work, the device will be used to analyse the causes and the parameters influencing the appearance of the buckles via parametric studies such as the tension of the membrane, the yarn geometry, the architecture of the fabric.

## 2. The tow buckle defect; parameters controlling its appearance

During the forming of particular complex shapes such as tetrahedron or prism the tow buckle defect may appear. This defect appears in specific zones of the formed shapes as shown in Fig. 1. On the tetrahedron, shape, the buckles appear on a localised zone converging to the top of the shape, and also on one of its edge [17]. As shown by Fig. 1, the tow buckling defect is characterised by an elevation of tows out of the plane of the fabric. The height of the buckles has been reported on the same study to be as high as 2 mm for the considered flax woven fabric. The size of the buckles is not homogeneous on the buckle's zone. As the defect is localised and its size not constant along the buckle's zone, the preform is therefore not homogeneous. As a consequence, the formed shape cannot be accepted. This defect has been reported by several authors for different types of textile architectures and different natures of tows within fabrics. Potter et al. [19] reported out of plane buckling of tows in a carbon woven fabrics. Beakou et al. [35] reported and modelled the appearance of tape buckling during the robot lay-up of carbon prepreg. Ouagne et al. [17,36], Allaoui et al. [37], showed that tow buckles appear in specific zones of complex shapes when flat based rectangular tows are used. The buckles were observed for flax based plain weave and twill weave fabrics and on interlock carbon fabric.

As described in the previous paragraph, the tow buckling defect may appear on laid up prepreg tapes as well as on tows within a fabric. Beakou et al. [35] modelled the appearance of defects anal-

ogous to the ones shown in Fig. 1 in the frame of prepreg tape lay-up. However, the appearance of tow buckles in woven fabrics is more complex. In the first studies reporting the appearance of the tow buckling defect during the forming process, the main mechanism without which the tow buckling defect cannot appear has been identified for different carbon, glass and flax flat tow based woven fabrics [17,36,37]. This mechanism is the bending in their plane of flat tows imposed by the geometry of the complex shape (Fig. 2). As this mechanism cannot be or can only be partially accommodated by the tow, another mechanism consisting in deforming the tow out of its plane takes place and a buckle as shown in Fig. 1 appears. The measurements performed on a face of a tetrahedron where tow buckling appears show that globally, the bending angles remain similar all along the buckling zone with lower values (more severe bending) towards the top of the shape. This bending angle quasi-continuity means that the displacements of the tows exhibiting the buckles are almost similar and symmetrical against the curvature point line shown in Fig. 2c.

However, the in-plane bending of the tow is not the only parameter influencing the appearance of the tow buckles. The tensile deformation of the tows perpendicular to the ones exhibiting the buckles was shown to be an important parameter to delay and reduce the magnitude of the buckles size. Ouagne et al. [38] showed that the tensile strains of the tows, situated in the buckle's zone, are the highest of the ones recorded on the different areas of the shape. Particularly, the deformations of the tows passing by the top of the tetrahedron shape are the highest ones, and the magnitude of the tensile deformation decreases as a function of the distance from this tow. As the buckles are situated in high tensile strain zones [39], blank holders to reduce the tension of the tows perpendicular to the ones showing the buckles were designed [8]. That study showed that it was possible to reduce the size of the buckles and to delay their appearance by reducing the tensile strains in the tows perpendicular to the ones showing the buckles. It is important to note that the deformation of the tows passing by the top of the tetrahedron depends on the architecture of the fabric. As an example, an un-balanced fabric does not show equivalent tensile strains in these tows for both warp and weft directions, and the magnitude of the buckle's size may be affected.

Ouagne et al. [7] showed that the appearance of buckles could be prevented on the face of the tetrahedron shape they studied by reducing the space between flat tows perpendicular to the ones exhibiting the buckles. In these conditions, the tow does not have a wide enough space to allow the development of a buckle. In the same work the authors showed that a hopsack fabric manufactured from cylindrical yarns did not exhibit any tow buckles. This means that the meso-architecture of the fabric is also very important and should be an important point of study.

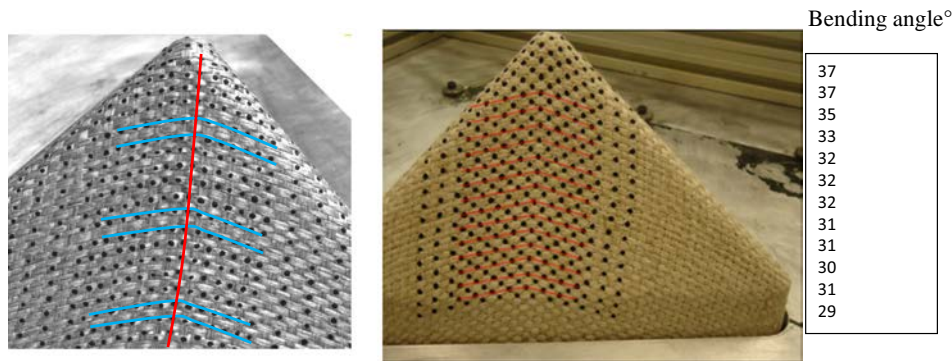


**Fig. 2.** (a) Bending of flat tows in their plane; (b) bending angle values. (For interpretation of the references to colour in this figure legend, the reader is referred to the web version of this article.)

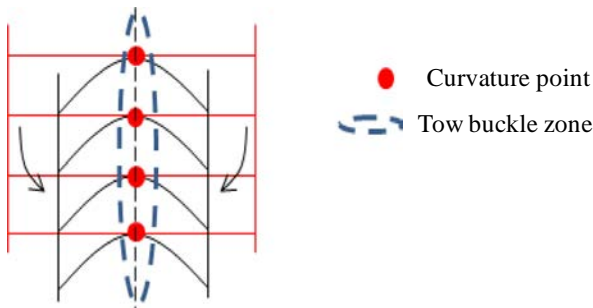


**Fig. 2c.** Principle of the tow in-plane bending during the forming process of a tetrahedron shape. (For interpretation of the references to colour in this figure legend, the reader is referred to the web version of this article.)

The previous paragraph therefore demonstrates that the appearance of tow buckles depends on multiple factors. As a consequence, the design of a device capable of reproducing independently of the forming process this defect should take into account all these parameters.

### 3. Design of the instrumented tow buckling device

As explained in Section 2, the causes influencing the appearance of tow buckles can be multiple. As a consequence, the device should be able to take into account separately the parameters already identified that may contribute to the appearance of tow buckles. The device should be able to impose a deformation capable to induce in-plane bending on tows expected to exhibit buckles, and to impose variable tensile loads on both directions.

An instrumentation associated to the mechanical device should also be considered carefully so that all the sensors that measure different quantities do not interact negatively between each other's. The movement of the jaws applying the in plane bending within the fabric should be measured and quantified. The loads imposed in both directions should also be measured as well as the tensile strains within the tows. Finally, the detection of the buckle's appearance as well as the measurement of the elevation kinematic of the defect needs to be evaluated accurately with a non-contact technique that should be able to be operational for any type textile architecture (woven fabrics mainly, non-crimped fabrics) and for any nature of the constituents (glass, carbon, aramid, natural fibres).

#### 3.1. Deformation kinematic for the buckling device

According to Section 2, the buckling defect is mainly the result of a combination between the bending of tows in their plane and

the level of tension applied to the tows perpendicular to the ones showing the buckles. The tension imposed to the tows showing the buckles is also probably very important and should also be studied. Fig. 2 shows that the tows exhibiting buckles bend in their plane according to a straight line imposed by the geometry of the shape to be formed. For any tow, only a bending point is observed, and the bending of tows is similar all along the height of the shape. The tows showing the buckles therefore remain parallel relatively to each other. The deformation can therefore be summarised by Fig. 3. Both directions of a woven fabric maintained by jaws are submitted to adjustable tension loads. To impose the bending deformation, the jaws in the direction 1 are then submitted to a circular translation without rotation of the local jaw basis. The circular translation has been preferred to a rotation because the rotation leads to an extension of the tows oriented in the Y direction on the upper part of the device and compression of the tows situated on the lower part leading to the appearance of a membrane wrinkle instead of tow buckles. Moreover, the length of the tows, the tension of the tows and their orientation would not be conserved in the case of a rotation. On the contrary, the circular translation implies that every segment of an object which follows this movement remains parallel to itself and that for every considered point of the object following a circular movement. As a consequence the lengths of the tows as well as parallel orientations between the tows are conserved. This circular translation can be performed by an assembly of connecting rod/pivot as shown by Fig. 4. The maximum circular angle translation of the device is 45°.

#### 3.2. Presentation of the buckling device

The experimental device presented in Fig. 4 is able to apply tensions in two directions. A first fixed axis applies a tension to tows originally perpendicular to the ones which are supposed to show buckles (Fig. 4a). On the tetrahedron preform (Fig. 2), these are the vertical tows. The second axis is constituted of two mobile jaws that perform a circular translation (Fig. 4b). The circular translation movement is conferred in each side of the mobile axis by two pivoting axis as shown in Fig. 4c. Those elements have been designed so that to prevent any out of plane bending of these two axes when tension loads are applied. Consequently two parallel bars have been placed (Fig. 4c, and e). The reinforcement is held in four zones between two thin steel plates (2 mm thick) as it is the case for the biaxial tension tests [29] placed within the jaws. Pressure screws impose a load on plates placed within the jaws. The jaws can slide on their support (fixed or mobile) and their movement is conferred by threaded rods for each direction (Fig. 4d). The loads can be measured by an in house made strain gage based sensor (Fig. 4d). The sensors measurement range is between 0 and 1 kN.

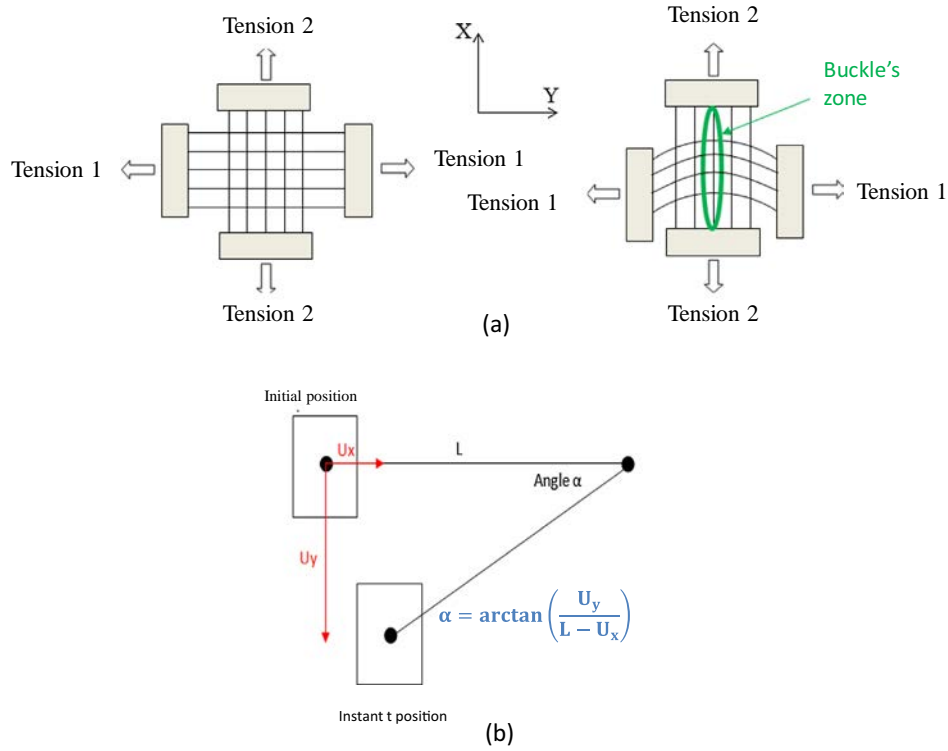


**Fig. 3.** (a) Principle of the tow buckling device; (b) measurement of the bending angle. (For interpretation of the references to colour in this figure legend, the reader is referred to the web version of this article.)

The displacement of the circular translation jaws is imposed by two threaded screws associated to springs to prevent the unwanted slack movements (Fig. 4e).

### 3.3. Device instrumentation

The device instrumentation aims to quantify the parameters that could be used to identify the phenomena associated to the buckles. Particularly, the height of the buckles, the circular displacement, the local tensile strains as well as the loads applied to the fabric should be evaluated carefully. All these parameters are measured simultaneously all along the test with the view to establish relationships between them and observe their relative influence on the tow buckling defect.

#### 3.3.1. Displacement of the mobile jaws and tensile strain measurement of the tows

The quantification of the mobile jaws' displacement is performed by two LVDT (Linear Voltage Displacement Transducer). A spring allows maintenance of a good contact between the mobile object and the sensor's rod. The respective displacements of both the LVDT's are  $\pm 25$  mm and  $\pm 10$  mm. This covers the maximum displacement permitted by the device. From the displacements given by the two LVDTs, the mobile jaw angle (or bending angle of the tows) can be evaluated as shown in Fig. 4b by Eq. (1).

$$\text{Bending angle} = \tan^{-1} \left( \frac{U_y}{L - U_x} \right) \quad (1)$$

where  $L$  is the distance between the centre of the buckling device and the centre of the mobile jaw,  $U_x$  and  $U_y$  are the displacements given by the two LVDTs as shown in Fig. 3b.

2D mark tracking technique is used to evaluate the tensile strains of tows. It is used to investigate the tensile strain evolution during a test [38]. It consists of following the displacement of

marks applied on chosen tows all along the test. Dots of paint applied manually can be followed by a digital camera placed perpendicular to the surface of the sample. A software (DEFTAC 2D) is then used to analyse the images taken during the test and calculate the displacements or strains between selected marks. This is a non-contact measurement technique that can be easily adapted to the buckling device. It is particularly interesting because it is possible to follow the tensile strain evolution of any tow, in the same time as the bending evolution of the tows in their plane.

#### 3.3.2. Tensile load measurements

The tensile loads are measured by in house manufactured sensors. These ones are based on strain gages placed on cylindrical rods that are deformed simultaneously of the screws applying the displacement. The strain gages via a balanced Wheatstone bridge provide compression or tension micro-deformation that can be recorded and converted to loads after a calibration procedure. The load sensors were calibrated in compression using an INSTRON 4411 universal testing machine in the range 0–1 kN using a calibrated 5 kN load cell before building the device.

#### 3.3.3. Geometry of the test samples

Several test sample geometries have been tested on the device to investigate if the tow buckles can be produced efficiently without any other side effect. Three geometries (square, cross, semi-cross) have been chosen and are presented in Fig. 5a.

The square geometry was quickly rejected as the movement of the mobile jaws leads to the formation of wrinkles which can be a problem for the measurement of the tow buckle's height. The cross geometry is the same as the one used for the biaxial tensile tests. With this geometry, the wrinkles disappear but tow sliding takes place on the upper part of the sample probably because of a lack of cohesion between the tows (Fig. 5b). The tow sliding is increased as a function of the applied tensions. This defect should be avoided

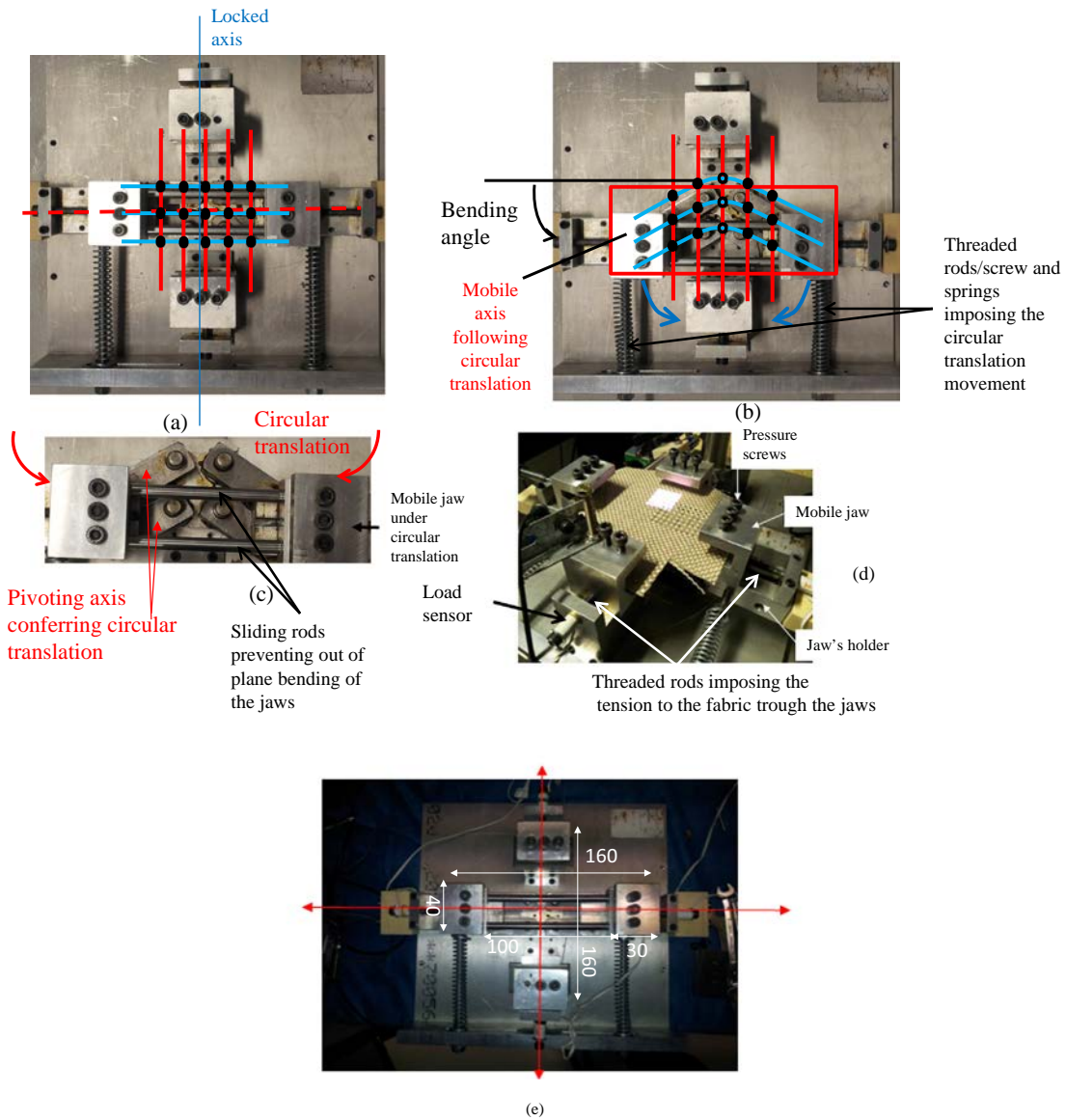


**Fig. 4.** Presentation of the buckling device mechanical part. (For interpretation of the references to colour in this figure legend, the reader is referred to the web version of this article.)

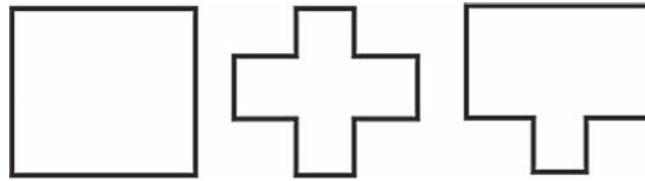
and prevented as the architecture of the reinforcement would be locally modified. This could change the mechanisms leading to the tow buckles and therefore, this geometry was also rejected. A semi-cross geometry (Fig. 5c) seems to be a good compromise between the two previous ones. It contains a larger quantity of material which prevents the tow sliding within the fabric and it does not lead to the formation of wrinkles in the bottom part. The tests are then performed by using this geometry with 160 mm \* 160 mm width and height, with squares of 40 × 40 mm<sup>2</sup> taken off in each side of the semi cross (Fig. 5c).

### 3.3.4. Measurement of the buckle's height

The detection of the buckles appearance as well as the measurement of its amplitude variation during its growth are critical parameters that need to be carefully and accurately measured. Particularly, the buckle's size, or buckle's height (Fig. 1) should be evaluated by a non-contact technique to avoid any interaction between the measurement and the buckle's appearance and growth.

In this work, the structured light interferometry technique has been used as it provides a resolution (~0.1 mm [40–42]) and a measurement surface that can be up to 1 m<sup>2</sup>. This method has also been chosen as it permits to follow continuously as a function of time the zone of interest. Stereo image correlation using 3D marks tracking was also considered, but it was rejected as the marks cannot be visible all along the elevation of the buckle.

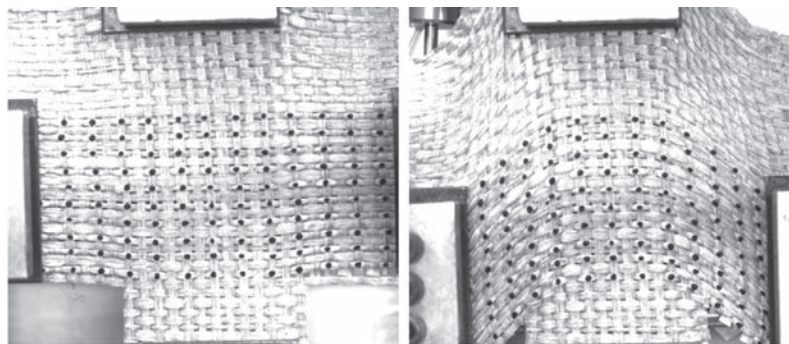
This interferometry technique is based on the projection of calibrated fringes (structured light). The technique requires a projector and a CCD camera. The principle of the method (Fig. 6), described in [43,44] consists in projecting alternative parallel black and white fringes on the object to examine. A CCD camera, positioned with an angle  $\theta$  relatively to the projection direction, records the image of the network deformed by the object. The optical phase difference, between the initial and the deformed network is related to the elevation of the plane to examine and it can be determined with accuracy for each pixel of the camera.



(a) Choice of geometry for the test samples



(b) Cross geometry: initial and final state



(c) Semi-cross geometry: initial and final state

**Fig. 5.** Test sample geometries.

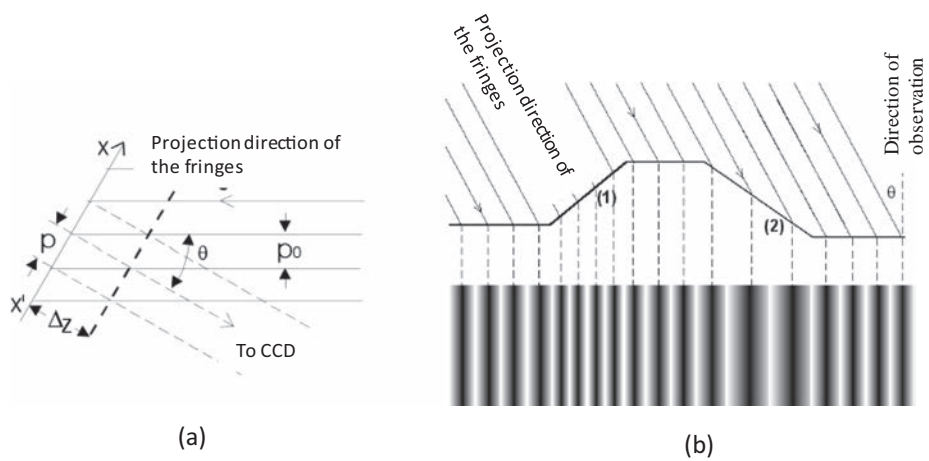


**Fig. 6.** Diagram of projected fringes: (a) on the plane of reference; (b) on a non planar profile.

## 4. Experimental procedure

### 4.1. Description of the used interferometry apparatus

The interferometry measurements have been performed at the SIMaP (Science et Ingénierie des Matériaux et Procédés) laboratory of Grenoble [45]. The used experimental device is composed of 3 main elements: a CCD camera, a video projector, and software elements H3SensorDigit3D coupled to the FringeAnalysis4<sup>®</sup>. The H3SensorDigit3D is a piece of software developed by the HOLO3 Company dedicated to the 3D digitalisation using optical ways. The FringeAnalysis4<sup>®</sup> is a software dedicated to the analysis of fringes images used in the holography, speckle or structured light interferometry. A video projector, is used to project calibrated computer elaborated fringes.

### 4.2. Materials

The reinforcement used in this study is a plain weave fabric manufactured by Groupe Depestele (France). The reinforcement is not balanced and is constituted of continuous rectangular untwisted yarns. The characteristics of the plain weave reinforcement are presented in Table 1(a). A twill weave fabric was also used in this work to manufacture calibrated buckles. This reinforcement is described in Table 1(b).

## 5. Results

### 5.1. Preliminary test

Before performing quantitative measurements, a preliminary test was performed on the  $2 \times 2$  twill weave fabric specific reinforcement with calibrated tow buckles defects manufactured and fixed by a spray of resin a priori to validate the technique and the data analysis. Fig. 7 shows that the size of the fringe projection zone is smaller than the size of the test sample. It is therefore important to know before a test where the buckles are supposed to grow. This is however not a problem since the buckles grow in a specific identified zone.

Large buckles from the twill weave fabric were used for this validation. Fig. 8 shows that the tows submitted to in plane bending (globally horizontal tows) and exhibiting the buckles show higher elevation than the vertical ones. It also shows that the height of the buckle is not homogeneous on a buckle's zone. It is possible to observe that the elevation is not equivalent along the width of a buckle. These observations are in good agreement with the ones

performed during the forming of the tetrahedron shape (Fig. 9). The buckle elevation is not uniform along its width and one side shows elevation whereas the other side does not.

### 5.2. Profile of the fabric and of the tow buckles

Firstly, a piece of the plain weave fabric is placed on the device with an orientation  $0^\circ$  as described by Fig. 10. The warp tows are the ones which are submitted to in-plane bending. The square periodic profile of elevation of a tow in the plain weave fabric is shown in Fig. 11a at the initial stage. The square profile is obtained even if measurement artefacts are observed. Fig. 11b shows the profile of altitude of the same zone at the final state of the test. This one differs from the idealised profile of tow buckles observed on one edge of a tetrahedron shape (Fig. 9b). The idealised profile of Fig. 11b shows that the buckles rise continuously on one side of their width.

#### 5.2.1. Profile of the buckles at the initial and at the final states

The profile of altitude along the  $X$ -axis has been recorded by the device for the studied reinforcement (Fig. 11). In Fig. 11, the profile of altitude is presented at the initial state (bending angle  $0^\circ$ ) and the final state (bending angle of  $42^\circ$ ). No tensile loads were applied in the direction perpendicular to the direction of the tow supposed to exhibit buckles. A clear variation of altitude can be observed between the initial and the final state, with elevations growing from about 0.4 mm up to 1.6 mm.

At the initial state, a square peak profile can be observed. Two different mean altitudes can be observed. These two altitudes correspond to the two directions of the tows within the fabric. Between two adjacent plateaus of higher elevation, lower altitudes can be observed. These lower altitudes are due to the fact that the tow perpendicular to the one exhibiting the buckles passes below it. On the measurements presented in Fig. 11a, the tows showing the higher plateaus are situated at an average elevations of  $0.39 \pm 0.03$  mm above the medium plane which is the reference elevation value  $0^\circ$ . The tows perpendicular to these ones are situated below the medium plane at a value of  $-0.11 \pm 0.04$  mm.

At the final stage, Fig. 11b shows that the profile of the peak changes between the initial and the final state and shows the spatial evolution of the tows. The peaks are characterised by a progressive rise of the elevation up to a maximum. After the maximum elevation point, a brutal drop of altitude is observed like in the buckle's profile presented in Fig. 9b for the formed tetrahedron shape. Before the peak, a compression phenomenon takes place. The tow exhibiting the buckle imposes a compression load on one of its side to the perpendicular tow as schematically represented in Fig. 12. On one side of the tow the point A presents a positive elevation. At the end of the buckle formation, the point A is situated at a maximum elevation. In the other side of the tow (point B) a negative elevation due to a compression of the tow on the perpendicular tow passing underneath it takes place. This phenomenon is the inverse consequence of the rise of the buckle. During the rotation of the tow around the  $Z$ -axis, another rotation around the  $Y$ -axis takes place. It is interesting to note that the axis of rotation around the  $Y$  axis is not situated in the middle of the tow. The width percentage of the tow in compression measured on the profile of the buckle (Fig. 11b) is of about 25%. One can also observe that the tows perpendicular to the ones exhibiting the buckles do not show a plateau anymore. They are characterised by a chevron profile which means that the lower elevation value is situated in a lower position than at the initial state:  $-0.4 \pm 0.2$  mm. The highest point of these tows is also situated at a lower elevation:  $-0.26 \pm 0.04$  mm. At the final state, one can also observe that the positions of the peaks are slightly translated in the

**Table 1**  
Reinforcements characteristics: (a) plain weave fabric; (b) twill weave fabric.

<i>(a) Plain weave fabric</i>		
Reinforcement composition	100% flax	
Manufactured by	Groupe Depestele (France)	
Reinforcement structure	Plain weave	
Yarn structure	Flat yarns	
Linear mass of yarns [tex]	Warp: $468.2 \pm 34.78$	Weft: $537.7 \pm 44.36$
Fabric areal weight ( $g/m^2$ )	$262 \pm 15$	
Average width of yarns (mm)	Warp: $2.12 \pm 0.35$	Weft: $2.46 \pm 0.28$
Average space between yarns	Warp $0.26 \pm 0.01$	Weft $1.59 \pm 0.09$
<i>(b) Twill weave fabric</i>		
Reinforcement composition	100% flax	
Manufactured by	Groupe Depestele (France)	
Reinforcement structure	Twill weave	
Yarn structure	Flat yarns	
Linear mass [tex]	Warp: $468.2 \pm 34.78$	Weft: $537.7 \pm 44.36$
Fabric areal weight ( $g/m^2$ )	$273 \pm 15$	
Average width of yarns (mm)	Warp: $2.4 \pm 0.4$	Weft: $2 \pm 0.4$
Average space between yarns	Warp: $0.9 \pm 0.2$	Weft: -

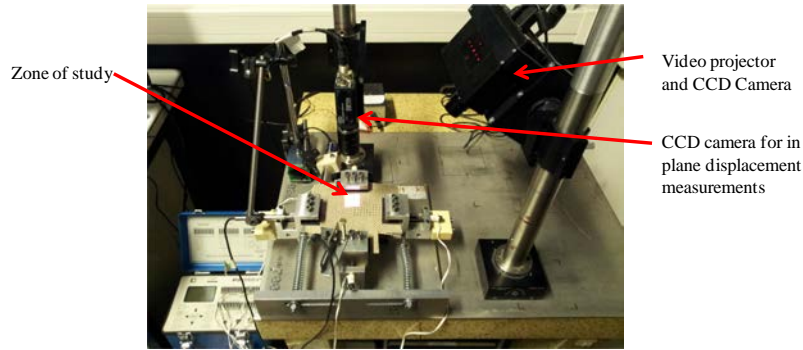


**Fig. 7.** Zone of study of the instrumented buckle's device. (For interpretation of the references to colour in this figure legend, the reader is referred to the web version of this article.)

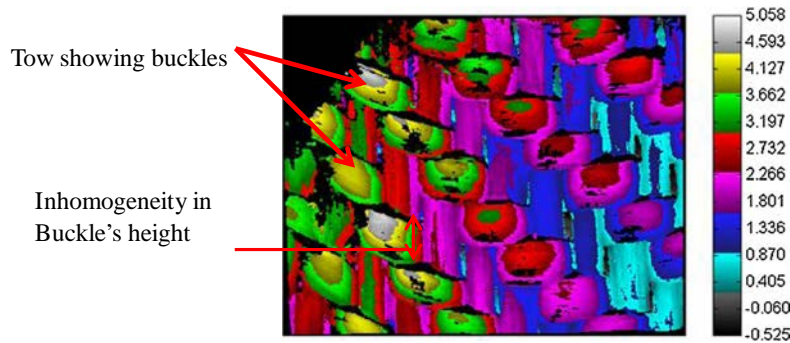


**Fig. 8.** Preliminary test on large tow buckles:  $2 \times 2$  twill weave fabric with fixed manufactured defects. (For interpretation of the references to colour in this figure legend, the reader is referred to the web version of this article.)

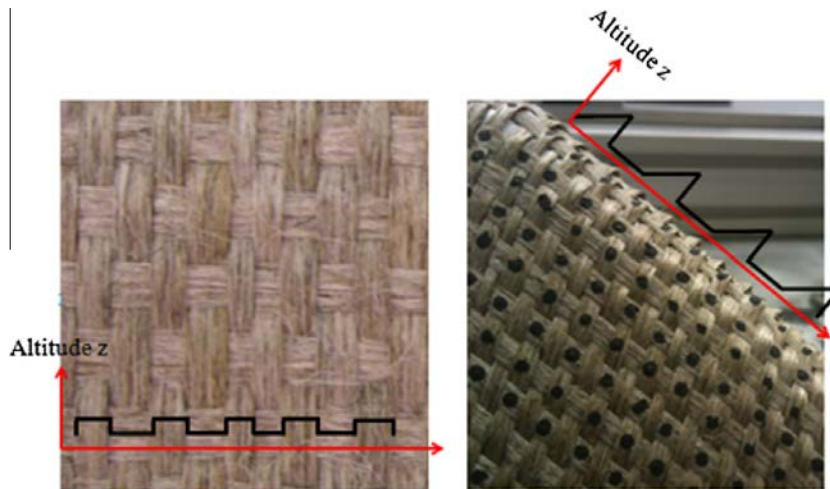


**Fig. 9.** Profile of altitude of a plain weave fabric (a); tow buckle's profile (b). (For interpretation of the references to colour in this figure legend, the reader is referred to the web version of this article.)

$x$ -direction. This is due to the displacement imposed to the fabric (and therefore to the tows) during the test.

At the initial state, some very important decreases of altitudes are observed after the peaks (Fig. 11a). These phenomena are probably the result of measurement artefacts due to the fact that the video projector light does not penetrate correctly in this particular zone and therefore, the altitude measurement is not correct.

Globally, the change of elevation between the maximum initial and final values of the tow exhibiting the buckles is within the range 1–1.2 mm. These results can be compared to measurements

carried out on the tetrahedron shape [7] with the same fabric. Globally a good correspondence can be observed between the results presented in this work and the ones presented in [7] for low blank holder pressure on the face of the tetrahedron where values of about  $1.1 \pm 0.1$  mm of elevation were recorded.

All the previous observations therefore indicate that the device is able to reproduce buckles with similar characteristics than the ones observed on the formed shape (Fig. 9) and also that the interferometry technique is completely adapted for the measurement of the buckle's elevation.

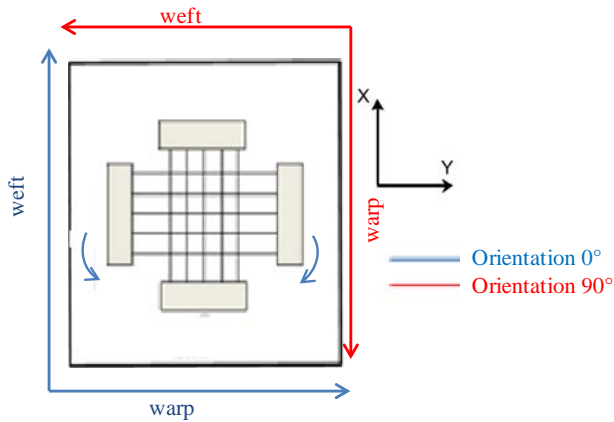


**Fig. 10.** Orientation of the fabric on the buckling device. (For interpretation of the references to colour in this figure legend, the reader is referred to the web version of this article.)

### 5.2.2. Evolution of the buckle's profile as a function of the bending angle

Fig. 13 shows the profile of altitude of tows 2 and 3 as defined in Fig. 11 as a function of the in-plane bending angle from the initial to the final state of the test. Each curve of the graph represents a different bending angle with an evolution of 1°. In Fig. 13a and c, the profile evolution is presented for bending angle situated within the 0–28° range. A progressive modification of the profile can be observed. However, up to the bending angle of 28°, the profile shows a quick rise of altitude followed by a plateau and a progressive drop of altitude. The drop of altitude becomes steeper for bending angles values of about 28°. If the profile remains globally similar, a rise of the plateau from an angle of about 20° is observed.

The altitude changes from a value of about 0.4 mm to a value of about 0.75 mm. A difference of 85% is observed.

Above 28° (Fig. 13b and d), the modification of the profile becomes more significant. The plateau situated after the initial rise of altitude progressively disappears and is replaced by a continuous rise of elevation up to the top of the buckle followed by a sudden drop. On the last bending angle variations, the profile no longer varies. One can therefore suppose that the buckle is completely formed and its growth stopped. This phenomenon takes place for an in-plane bending angle of about 40°. Fig. 14 summarises the evolution of the elevation as a function of the bending angle.

Comparisons with bending angles measured on the face of a tetrahedron presenting tow buckles [7] with similar elevations to the ones measured in this work indicate that the bending angles are situated in the range 35–42° for low blank-holder pressures. Once again, the measurements performed with the device are in good agreements with measurements performed at the end of the forming process with similar conditions.

The elevation of the buckles at the final state is of about  $1.6 \pm 0.2$  mm above the medium plane of the fabric. This value should then be compared to the width of the tow (2.12 mm). This means that the tow is capable to reach an elevation corresponding to about 75% of its width. The other part is situated below the medium plane and represents the part that imposes a compression load on the perpendicular tow.

## 6. Discussion: preliminary criterion for buckle appearance

In previous works [7,8,17,37], the in-plane bending of the tow exhibiting the buckle was identified as the main mechanism at the origin of the tow buckling defect. In these studies, the tow buckling defect was appearing as a result of the complex shape

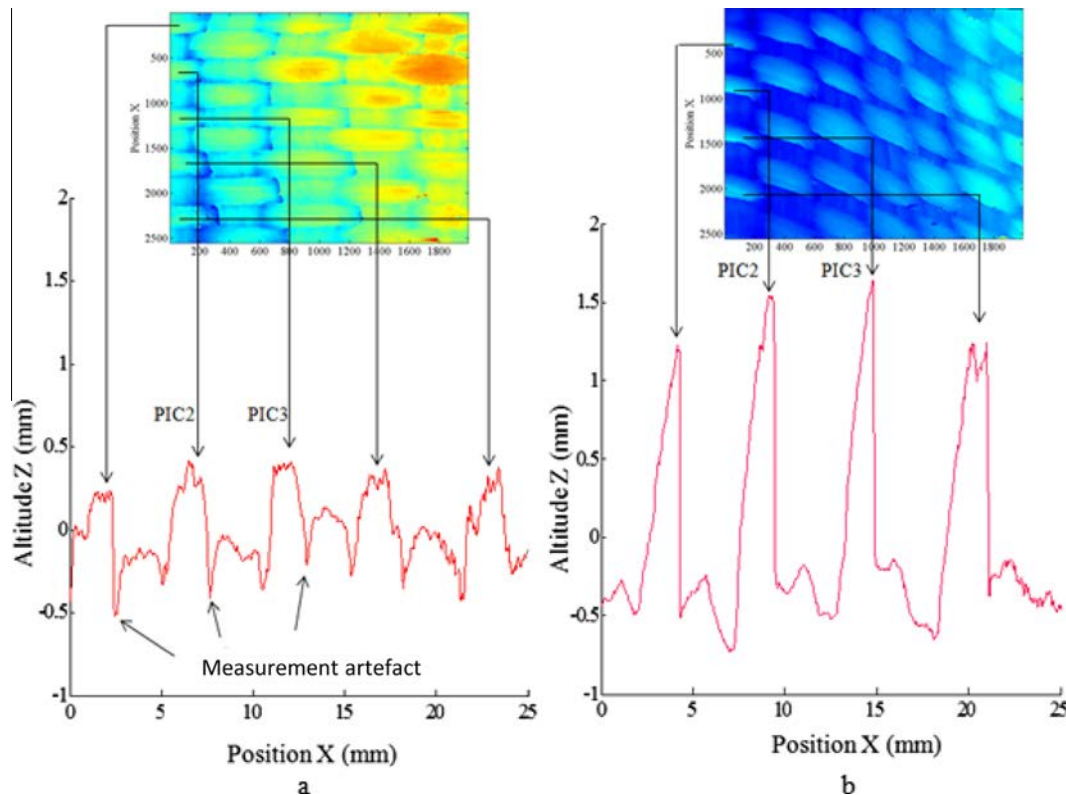


**Fig. 11.** Elevation profile for the plain weave fabric: initial state (a); final state (b). (For interpretation of the references to colour in this figure legend, the reader is referred to the web version of this article.)

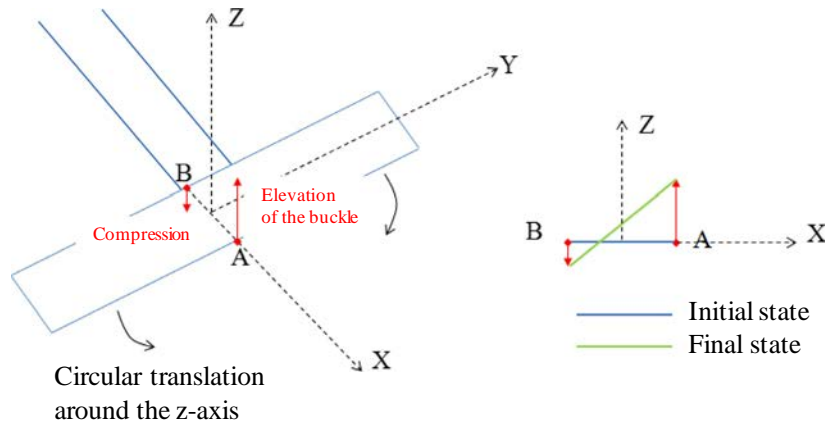


**Fig. 12.** Schematic diagram of the tow buckling appearance and growth. (For interpretation of the references to colour in this figure legend, the reader is referred to the web version of this article.)

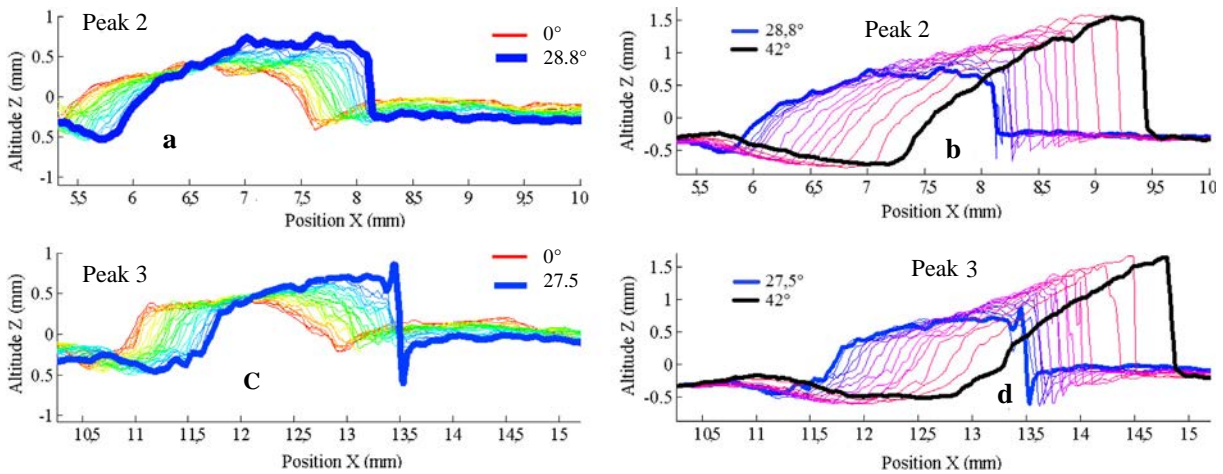


**Fig. 13.** Profile evolution of the tow exhibiting the buckle for increasing in-plane bending angles. (For interpretation of the references to colour in this figure legend, the reader is referred to the web version of this article.)

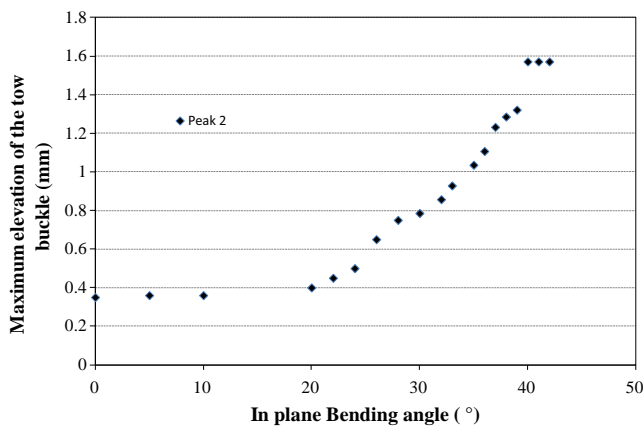


**Fig. 14.** Evolution of the maximum elevation of the tow buckle as a function of the in plane bending angle. (For interpretation of the references to colour in this figure legend, the reader is referred to the web version of this article.)

forming of woven fabrics. It was observed that several process parameters such as the tension in tows perpendicular to the ones exhibiting the buckles, as well as meso-structural parameters such as the width between tows perpendicular to the ones showing buckles influenced the appearance of the buckle. This study there-

fore aims to design a device capable to impose in plane bending to tows so that buckles can be produced. By observing the movement of the tows on the faces and edges of the tetrahedron, one can see that the tows when bending in their plane globally follow a circular translation even if it may not be a perfect one. During the process, the bending of the tows exhibiting the buckles is probably due to more complex combinations of movements within the textile structure, but the goal of this preliminary study is to produce buckles independently of the process by imposing a movement as close as possible to the real phenomenon.

A device designed to reproduce the tow buckling phenomenon was used to characterise into more details the conditions of appearance of the defect. A specific instrumentation was chosen to accurately measure the different parameters that could control the appearance of the tow buckle defect. Particularly, structure light interferometry was used to measure during all the duration of a test the variation of elevation of the tows. The same plain weave fabric already used in previous studies [7,8,17] was considered for this study.

This work of a preliminary nature concentrates on the appearance and on the growth of the buckle for one unique case of fabric loading. It was showed that a minimum in-plane bending angle (about 20° in our case) was necessary to observe a global elevation of the whole tow surface. Above a bending value of about 28°, the profile of the tow changes and the tow becomes submitted to a double rotation process. One rotation takes place around the Z axis, and another one takes place around the Y axis. As a consequence,

one side of the tow rises progressively whereas the other side drops progressively. About 75% of the width of the tow rises whereas about 25% drops. This proportion probably depends on the bending stiffness of the tow that partially controls the rotation around the Z-axis as well as the edge compression stiffness of the tow imposing the compression load and the surface compression stiffness of the perpendicular tow submitted to the load.

This work therefore shows that the appearance of a tow buckles takes place in several steps and mainly depends on the value of the in-plane bending angle. Fig. 14 shows the maximum elevation of the tow exhibiting the buckle. Below a value of about 20°, no elevation of tows is observed. Between 20° and 28°, the tow surface homogeneously rises of about 85% elevation. Above 28°, the tow buckle itself appears. A differential elevation is observed in both sides of the tow, and the plateau of elevation of the tow progressively transforms itself to continuous increase of elevation from one side of the tow to the other one as a result of a double rotation followed by the tow. A minimum bending angle is therefore required for a tow buckle to appear. Above a maximum in-plane bending angle (40° in our case of study), the buckle does not grow anymore. A maximum buckle size is therefore reached for a given tow width in a given pattern. The three steps just described indicate that the in-plane bending of the tow is the key parameter at the origin of the tow buckling defect. The critical in-plane bending angles values given in this work for the case of study exposed could however be modified as a function of other external parameters such as the tension imposed to the fabrics or internal structural parameters of the fabric. These values, could also be criticised as the buckles produced in this work are the result of the in plane bending of tows imposed by a circular translation. During the process, more complex combination of movements leading to in plane bending of tows showing the buckles within the fabric structure probably takes place. The appearance bending angle could therefore be different during the process than when using the buckling device. However, this work shows that bending angles necessary to produce tow buckles are in good agreement with previous studies where these parameters were measured directly on tetrahedron faces [7]. The growth evolution of the buckle with the double rotation may however be different during the process and during the production of tow buckles by the device. During the process, the fabric is in contact with the punch imposing the shape whereas the reinforcement is not in the case of the buckling device. In this case, the compression load described in this work may be different than during the draping process. However, this phase might not be critical as the size of the buckles produced by using the device are in very good agreement with the size of buckles measured after draping the same fabric in the tetrahedron face [7]. By imposing larger tensile loads on the tows perpendicular to the ones exhibiting the buckles, the compression phenomenon that takes place during the double rotation of the tow in the buckling zone could be therefore changed and be closer to the real draping situation.

As this work is of a preliminary nature, the influence of parameters such as the tension of the tows in both directions is not presented in this work. The influence of the meso-structure (nature of the pattern, size of the tow, width between tows, etc.) should also be investigated. The nature and of course the mechanical stiffnesses associated to the tow exhibiting the buckles should also be studied to investigate their respective influence on the buckle's appearance. All these investigations will have for goal to propose a model describing the tow buckle appearance.

## 7. Conclusions

With the view to investigate the tow buckling defect independently of the process, a device capable to reproduce the defect

was designed and associated to a specific instrumentation. Particularly, structure light interferometry was chosen to measure the elevation of the tows exhibiting the buckling defect all along its growth. The device and its instrumentation were validated in this work and a preliminary study was performed to investigate the origin of the tow buckle's appearance and its growth kinematic. It was shown that the in-plane bending of the tow is a key parameter controlling the appearance of the defect and its growth up to a maximum elevation above the medium plane of the fabric that is controlled by the geometry of the tow but also by its respective stiffnesses (bending and compression). This parameter can probably be considered as a preliminary criterion that conditions the appearance and the growth of the tow buckling defect. The growth kinematic of the buckle's appearance consisting on a double simultaneous rotation of the tow exhibiting the buckle around the Z and the Y axis was established. Due to the rotation of the tow around the Y-axis, one side of the tow imposes a compression load to the perpendicular tow. As a consequence, the profile of this tow changes from a square profile to chevron profile.

This work even if of a preliminary nature establishes a criterion conditioning the appearance and describes the progressive growth of the tow buckling defect. This work also establishes the basis necessary for a wider study of all the parameters that may influence the appearance and growth of the tow buckling defect by using the device and its specific instrumentation designed and exposed in this work.

## Acknowledgements

The authors would like to thank the ADEME – France (French Environmental agency) and Region Centre for their financial support. The authors also would like to thank the SIMaP laboratory of Grenoble for the use of their interferometry equipment.

## References

- [1] Wang P, Hamila N, Boisse P. Thermoforming simulation of multilayer composites with continuous fibres and thermoplastic matrix. *Composites Part B* 2013;52:127–36.
- [2] Liang B, Hamila N, Peillon M, Boisse P. Analysis of thermoplastic prepreg bending stiffness during manufacturing and of its influence on wrinkling simulations. *Composites: Part A* 2014;67:111–22.
- [3] Gereke T, Döbrich O, Hübner M, Cherif C. Experimental and computational composite textile reinforcement forming: a review. *Composites: Part A* 2013;46:1–10.
- [4] Chen S, Endruweit A, Harper LT, Warrrior NA. Inter-ply stitching optimisation of highly drapeable multi-ply preforms. *Composites: Part A* 2015;71:144–56.
- [5] Allouai S, Cellard C, Hivet G. Effect of inter-ply sliding on the quality of multilayer interlock dry fabric preforms. *Composites: Part A* 2015;68:336–45.
- [6] Smerdova O, Sutcliffe MPF. Multiscale tool-fabric contact observation and analysis for composite fabric forming. *Compos Part A: Appl Sci Manuf* 2015;73:116–24.
- [7] Ouagne P, Soulat D, Moothoo J, Capelle E, Gueret S. Complex shape forming of a flax woven fabric; analysis of the tow buckling and misalignment defect. *Composites Part A* 2013;51:1–10.
- [8] Capelle E, Ouagne P, Soulat D, Duriatti D. Complex shape forming of flax woven fabrics: design of specific blank-holder shapes to prevent defects. *Composites Part B* 2014;62:29–36.
- [9] Pazmino J, Mathieu S, Carvelli V, Boisse P, Lomov SV. Numerical modelling of forming of a non-crimp 3D orthogonal weave E-glass composite reinforcement. *Composites: Part A* 2015;72:207–18.
- [10] Dufour C, Wang P, Boussu F, Soulat D. Experimental investigation about stamping behaviour of 3D warp interlock composite preforms. *Appl Compos Mater* 2014;21(5):725–38.
- [11] Peng X, Guo Z, Diu T, Yu WR. A simple anisotropic hyperelastic constitutive model for textile fabrics with application to forming simulation. *Composites Part B* 2013;52:275–81.
- [12] Hamila N, Boisse P. Locking in simulation of composite reinforcement deformations. Analysis and treatment. *Composites: Part A* 2013;53:109–17.
- [13] Bloom LD, Wang J, Potter KD. Damage progression and defect sensitivity: an experimental study of representative wrinkles in tension. *Composites: Part B* 2013;45:449–58.
- [14] Lee J, Hong S, Yu W, Kang T. The effect of blank holder force on the stamp forming behavior of non-crimp fabric with a chain stitch. *Compos Sci Technol* 2007;67:357–66.

- [15] Lin H, Wang L, Long AC, Clifford MJ, Harrison P. Predictive modelling for optimization of textile composite forming. *Compos Sci Technol* 2007;67:3242–52.
- [16] Boisse P, Hamila N, Vidal-Sallé E, Dumont F. Simulation of wrinkling during textile composite reinforcement forming. Influence of tensile, in-plane shear and bending stiffnesses. *Compos Sci Technol* 2011;71(5):683–92.
- [17] Ouagne P, Soulat D, Hivet G, Allaoui S, Duriatti D. Analysis of defects during the preforming of a woven flax. *Adv Compos Lett* 2011;20:105–8.
- [18] Gatouillat S, Bareggi A, Vidal-Sallé E, Boisse P. Meso modelling for composite preform shaping. Simulation of the loss of cohesion of the woven fibre network. *Composites Part A* 2013;54:135–44.
- [19] Potter K, Khan B, Wisnom M, Bell T, Stevens J. Variability, fibre waviness and misalignment in the determination of the properties of composite materials and structures. *Composites: Part A* 2008;39:1343–54.
- [20] Walther J, Simacek P, Advani SG. The effect of fabric and fiber tow shear on dual scale flow and fiber bundle saturation during liquid molding of textile composites. *Int J Mater Form* 2012;5:83–97.
- [21] Vernet N, Ruiz E, Advani S, et al. Experimental determination of the permeability of engineering textiles: benchmark II. *Compos Part A: Appl Sci Manuf* 2014;61:172–84.
- [22] Ouagne P, Bréard J. Continuous transverse permeability of fibrous media. *Composites: Part A* 2010;41:22–8.
- [23] Ouagne P, Ouahbi T, Park C-H, Bréard J, Saouab A. Continuous measurement of fiber reinforcement permeability in the thickness direction: experimental technique and validation. *Composites: Part B* 2012;45:609–18.
- [24] Van Den Brouck B, Hamila N, Middendorf P, Lomov SV, Boisse P, Verpoest I. Determination of the mechanical properties of textile-reinforced composites taking into account textile forming parameters. *Int J Mater Form* 2010;3(Suppl 2):S1351–61.
- [25] Hamila N, Boisse P. Simulations of textile composite reinforcement draping using a new semi-discrete three node finite element. *Composites: Part B* 2008;39:999–1010.
- [26] Boisse P, Zouari B, Daniel JL. Importance of in-plane shear rigidity in finite element analyses of woven fabric composite preforming. *Composites Part A* 2006;37(12):2201–12.
- [27] Cao J et al. Characterization of mechanical behavior of woven fabrics: experimental methods and benchmark results. *Composites: Part A* 2008;39:1037–53.
- [28] Hivet G, Boisse P. Consistent mesoscopic mechanical behaviour model for woven composite reinforcements in biaxial tension. *Composites: Part B* 2008;39:345–61.
- [29] Gasser A, Boisse P, Hanklar S. Mechanical behaviour of dry fabric reinforcements. 3D simulations versus biaxial tests. *Comput Mater Sci* 2000;17: 7–20.
- [30] de Bilbao E, Soulat G, Launay D, Hivet J, Gasser A. Experimental study of bending behaviour of reinforcements. *Exp Mech* 2010;50(3):333–51.
- [31] Allaoui S, Hivet G, Wendling A, Ouagne Soulat P. Influence of the dry woven fabrics meso-structure on fabric/fabric contact behavior. *J Compos Mater* 2012;46(6):627–39.
- [32] Ten Thije RHW, Akkerman R, Ubbink M, et al. A lubrication approach to friction in thermoplastic composites forming processes. *Compos Part A: Appl Sci Manuf* 2011;42:950–60.
- [33] Walid Najjar W, Pupin C, Legrand X, Boude S, Soulat D, Dal Santo P. Analysis of frictional behavior of carbon dry woven reinforcement. *J Reinforced Plastics Compos* 2014;33(11):1037–47.
- [34] Arbter R, Beraud JM, Binetruy C, Bizet L, Bréard J, Comas-Cardona S, et al. Experimental determination of the permeability of textiles: a benchmark exercise. *Composites Part A* 2011;42:1157–68.
- [35] Beakou A, Cano M, Le Cam JB, Verney V. Modelling slit tape buckling during automated prepreg manufacturing: a local approach. *Compos Struct* 2011;93(10):2628–35.
- [36] Ouagne P, Soulat D, Allaoui S, Hivet G. Mechanical properties and forming possibilities of a new generation of flax woven fabrics. In: *Proceeding of the 10th international conference on textile composite (Texcomp)*. Lille; 26–28 October 2010.
- [37] Allaoui S, Hivet G, Soulat D, Wendling A, Ouagne P, Chatel S. Experimental preforming of highly double curved shapes with a case corner using an interlock reinforcement. *Int J Mater Form* 2014;7(2):155–65.
- [38] Ouagne P, Soulat D, Tephany C, Duriatti D, Allaoui S, Hivet G. Mechanical characterisation of flax based woven fabrics and in situ measurements of tow tensile strain during the shape forming. *J Compos Mater* 2013;47(28):3498–512.
- [39] Ouagne P, Soulat D, Tephany C, Moothoo J, Allaoui S, Hivet G, et al. Complex shape forming of flax based woven fabrics. Analysis of the yarn tensile strain during the process. *Key Eng Mater* 2012;504–506:231–6.
- [40] Ibrahim ME. Nondestructive evaluation of thick-section composites and sandwich structures: a review. *Compos Part A: Appl Sci Manuf* 2014;64:36–48.
- [41] Devivier C, Pierron F, Wisnom MR. Damage detection in composite materials using deflectometry, a full-field slope measurement technique. *Compos Part A: Appl Sci Manuf* 2012;43(10):1650–66.
- [42] Pieron F. Application of full-field measurement techniques to composite materials and structures. *Compos Part A: Appl Sci Manuf* 2008;39(8):1193.
- [43] Theocaris PS. *Moiré fringes in strain analysis*. Elmsford: Pergamon Press; 1969.
- [44] Post D, Han B, Ifju P. *High sensitivity moiré: experimental analysis for mechanics and materials*. Berlin: Springer; 1994.
- [45] <http://simap.grenoble-inp.fr/accueil/>.